

# CrystEngComm

Accepted Manuscript



This is an *Accepted Manuscript*, which has been through the Royal Society of Chemistry peer review process and has been accepted for publication.

*Accepted Manuscripts* are published online shortly after acceptance, before technical editing, formatting and proof reading. Using this free service, authors can make their results available to the community, in citable form, before we publish the edited article. We will replace this *Accepted Manuscript* with the edited and formatted *Advance Article* as soon as it is available.

You can find more information about *Accepted Manuscripts* in the [Information for Authors](#).

Please note that technical editing may introduce minor changes to the text and/or graphics, which may alter content. The journal's standard [Terms & Conditions](#) and the [Ethical guidelines](#) still apply. In no event shall the Royal Society of Chemistry be held responsible for any errors or omissions in this *Accepted Manuscript* or any consequences arising from the use of any information it contains.

## ARTICLE

Cation Exchange of Aqueous CuInS<sub>2</sub> Quantum Dots

Cite this: DOI: 10.1039/x0xx00000x

Thomas J. Macdonald<sup>a,c†</sup>, Yatin J. Mange<sup>a,c†</sup>, Melissa Dewi<sup>a,c</sup>, Aoife McFadden<sup>b</sup>, William M. Skinner<sup>a</sup>, Thomas Nann<sup>a,c\*</sup>Received 00th January 2012,  
Accepted 00th January 2012

DOI: 10.1039/x0xx00000x

www.rsc.org/

Chalcopyrite copper indium disulfide (CIS) QDs have been of recent interest due to their non-toxicity. Although publications on CIS QDs are becoming more common, the majority of synthesis involves long chained insulating ligands, which are only soluble in non-polar solvents. Recent workers have explored the tunable properties of CIS QDs by means of cation exchange with ZnS. Despite this, their tunable properties have been limited to use in organic solvents. This may be due to the cation exchange not being completely understood. For the first time, we present a controllable cation exchange for water soluble, tunable CIS QDs. We also show the partial exchange of indium for zinc, which is shown to provide these QDs with unique optical properties.

## Introduction

Quantum dots (QDs) are semiconducting nanocrystals whose excitons are confined in all three spatial dimensions. Chalcopyrite copper indium disulfide (CIS) QDs have been of recent interest due to their non-toxic credibility and their absorption/luminescence characteristics in the UV-visible range of the electromagnetic spectrum. Although publications on CIS QDs are becoming more common, most synthesis routes are based on long chained alkyl ligands, which are only soluble in non-polar solvents.<sup>1</sup> Reports on the growth of a passivating shell or cation exchange for CIS QDs is quite rare.<sup>1-4</sup> In this study, we present an aqueous synthesis method for CIS QDs, followed by a controllable cation exchange that also tunes the optical properties of the particles. Furthermore, we show how these QDs can be used as sensitizers for *n-type* semiconductors for water-splitting and solar cell applications.

Non-toxic and toxic QDs are commonly synthesized with high-boiling, non-polar solvents such as 1-octadecene (ODE). These solvents contain non-polar ligands, and thus are dispersible only in non-polar compounds such as hexane, toluene or chloroform.<sup>2-5</sup> Typically, these organic molecules must be removed from the QDs for applications such as solar cells, due to their insulating effect. While there has been published work on exchanging bulky organic ligands and solvents with hydrophilic alternatives,<sup>6-8</sup> it still remains a challenging process. Synthesizing QDs in an aqueous solvent reduces purification and post-synthesis modification steps making it an easier, cheaper and more desirable synthesis over conventional organic routes.

The synthesis of tertiary chalcopyrite materials such as CIS were reported as early as 1998.<sup>9</sup> The synthesis employed techniques including thermolysis,<sup>10</sup> photochemical deposition,<sup>11</sup> and to achieve monodispersity, the hot-injection method.<sup>12</sup> CIS QDs have proven to be a promising compound exhibiting good light-absorbing characteristics.<sup>13</sup> CIS has a direct band gap of 1.45 eV which is equivalent to a 850 nm wavelength.<sup>1</sup> Initially,

CIS quantum dots commonly show poor luminescence and very broad photoluminescence spectra. This is generally indicative of a polydisperse distribution of nanoparticles. Recent work on CIS QDs has found methods to increase quantum yields, increase photoluminescence intensities,<sup>14</sup> investigate their tunable properties<sup>2</sup> and alter the size of the nanoparticles.<sup>15</sup> This has been achieved by introducing zinc and surface capping ligands such as oleylamine. By introducing zinc to the synthesis, a ZnS shell was grown on the core of the CIS QDs. Typically, the addition of a shell such as zinc sulfide for cadmium based QDs results in an emission shift to the red. This is most likely due to an increase in QD core size by adding a thicker shell around the core.<sup>16</sup> Similar techniques have been used with CIS QDs. However, a luminescence shift to the blue was observed, which may have been caused by exchange of CIS cations with zinc and thereby “shrinking” of the actual QD core.<sup>2</sup>

This effect has been observed before and the reason has been attributed to three possible scenarios. First, Reiss *et al.* suggested the possibility of surface reconstruction,<sup>17</sup> second, the inter-diffusion of Zn atoms was reported by Pons *et al.*,<sup>1</sup> and third, Park *et al.*,<sup>4</sup> attributed the blue shift to a cation exchange on the surface of the CIS. These studies lead to the suggestion that CIS/ZnS QDs could be synthesized with emission colors ranging from the red to the near blue region by partial cation exchange without altering the size of the QDs.<sup>4,18</sup> The emission properties of CIS/ZnS are generally tunable from the yellow to the red<sup>19</sup> with the one exception published by Peng *et al.*, where the optical properties resemble those of CdSe QDs.<sup>20</sup>

With the exception of CdTe, achieving a tunable quantum dot synthesis in an aqueous solvent has yet to be published. For the first time we present an aqueous synthesis route for CIS/ZnS QDs via a controlled cation exchange, which provides unique optical properties. In this article, we will show that the ZnS layer formed by cation exchange does not form a well defined shell, but a gradual increase in Zn from the core to the

shell. Therefore, the nomenclature of core/shell might be misleading, but we keep this terminology here to conform with other publications in this field.

## Results

Aqueous CIS QDs were synthesized using a modification of the methodology reported by Meng *et al.*<sup>21</sup> In this modification, the acidic solution was neutralized using NaOH and subsequent aliquots of 20, 30, 40, and 50 mg of zinc acetate were added.

### Spectroscopy

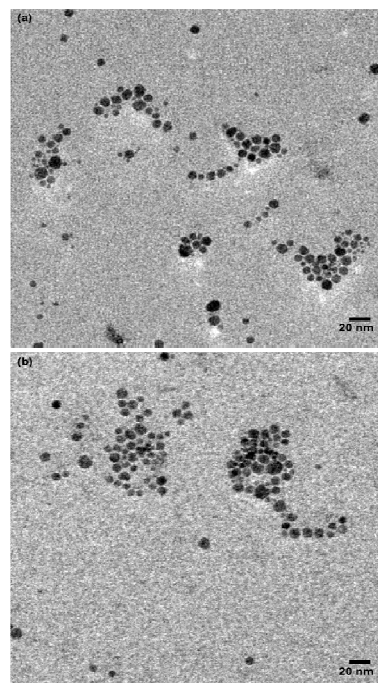
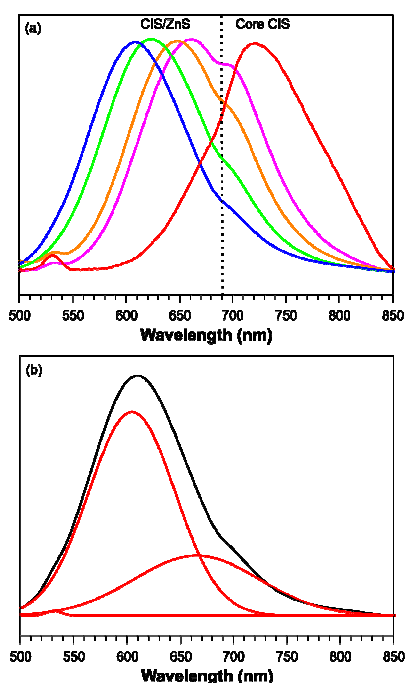
The amounts of zinc acetate were varied to determine the relationship between the ionic salt and the aqueous QDs. Excess amounts of salt resulted in aggregation of the QD solutions, which is probably due to a break down of the electrostatic double layer ("salting the colloid out"). Figure 1 shows the emission spectra of the CIS QDs for both the core and the zinc treated QDs. Strong emission peaks may be seen from 610 through to 725 nm. Within this wavelength range a blue shift of 115 nm was observed; 30 nm higher than that ever reported for CIS QDs previously.<sup>22</sup> The full width at half maximum (FWHM) was measured to be approximately 110 nm. To our knowledge this is the narrowest FWHM photoluminescence peak for aqueous CIS QDs. This FWHM is in accordance with values obtained for CIS QDs prepared with the well-established organic synthesis method, that have undergone a treatment with zinc.<sup>23</sup> To ensure that the blue shift was not caused by using zinc acetate, Park *et al.*,<sup>4</sup> examined this shift using different zinc precursors including, zinc chloride, zinc stearate and zinc acetylacetonate. They found that the type of zinc source could not be correlated to the blue shift. However, they did find that zinc stearate produced the largest blue shift of 80 nm, which is 35 nm lower than our largest shift with zinc acetate (115 nm). Since our synthesis was in the aqueous phase we chose to use zinc acetate which was the second most effective precursor (after zinc stearate) for the blue shift recognized in the work by Park *et al.*<sup>4</sup> Quantum yields of ~ 1% have been measured for the CIS QDs.

**Figure 1:** (a) Photoluminescence emission spectra for CIS/ZnS QDs, (b) Gaussian distribution for CIS/ZnS emission at 5 mM Zn-acetate

The emission peaks show a shoulder at approximately 690 nm. This has been seen before and attributed to the inhomogeneity of the QDs.<sup>22</sup> There is also a lower emission shoulder (defect) which may be seen at around 535 nm. This is most dominant in the core CIS QDs. Interestingly, we can see that upon the addition of zinc this defect is significantly reduced and appears to be gone once 5 mM zinc acetate is added. There is little knowledge about these defect sites given the small size of the QDs, however Manna *et al.*, suggest that the reduction of lower energy emission shoulders<sup>22</sup> is due to Zn passivation of donor defect sites in the CIS lattice. They also put forward two hypotheses; firstly, Zn may be filling copper vacancy sites or secondly, expulsion of interstitial atoms is occurring during cation exchange. In addition, figure 1b) shows a Gaussian distribution for the photoluminescence peaks. Since the emission peaks at 535 and 690 nm do not shift when zinc is added to the solution, this supports the hypothesis that these peaks may be caused by defect states. The defect states have been reported before. Whilst we recognize this, further work is required to confirm Zn is filling the vacancies.

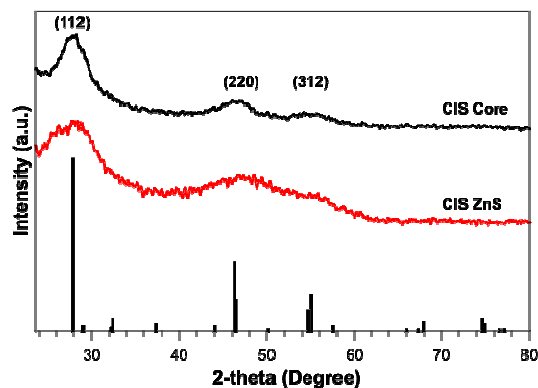
### XRD and TEM

The tunable properties of the CIS QDs can be correlated to a partial cation exchange of copper or indium with zinc. Most studies on CIS QDs and their tunable properties with metal ions such as zinc, attribute the photoluminescence shift to particle size changes.<sup>17,24</sup> The particle sizes in the present study were measured using transmission electron microscopy (TEM) (Figures 2a and b), and exhibit a similar size distribution for both core and zinc exchanged CIS particles.



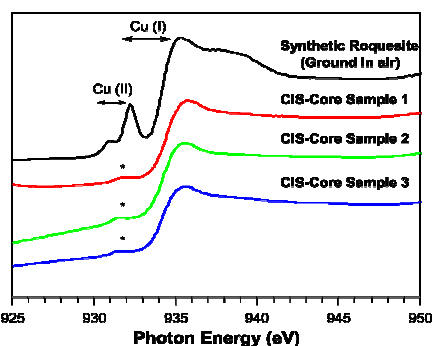
**Figure 2:** TEM micrographs of (a) CIS and (b) CIS/ZnS QDs

The crystalline structure of the QDs was also investigated using X-ray diffraction (XRD). The patterns obtained from the XRD are shown in Figure 3. The three broad diffraction peaks are located at 28, 46, and 55 (2 $\theta$ ), which agrees with the crystalline structure and JCPDS-file 00-047-1372 for the natural mineral roquesite, CuInS<sub>2</sub>.

**Figure 3:** XRD 2 $\theta$  traces for core CIS and CIS/ZnS QDs. Bars represent reflections according to JCPDS-file 00-047-1372 for roquesite, CuInS<sub>2</sub>.

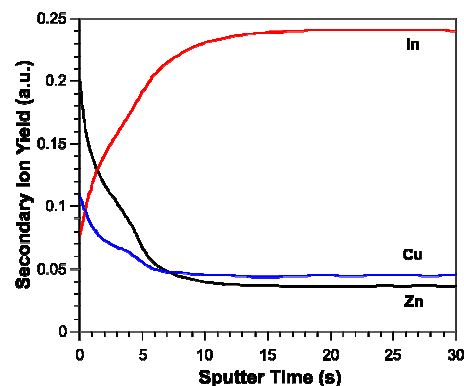
#### NEXAFS, ToF-SIMS and XPS

Cu L<sub>3</sub>-edge near-edge X-ray absorption fine structure (NEXAFS) and synchrotron-based XPS (SXPS) measurements were performed on CIS nanoparticles with adsorbed ligands, and synthetic CuInS<sub>2</sub> (roquesite) ground in air. The latter was analyzed as a standard that exhibited both the synthetic bulk CIS edge structure, together with a reference for CIS oxidation products – specifically Cu(I) and Cu(II) surface species (typically Cu oxides and hydroxides). Cu 2p SXPS showed no indication of Cu(II) on the surfaces of the CIS nanoparticles, due to the absence of characteristic Cu(II) excited final state (shake-up) satellites.<sup>25</sup> The Cu L<sub>3</sub> absorption edge is approximately 25 times more sensitive to Cu(II) than Cu(I), due to increased d-like state vacancies. The Cu L<sub>3</sub>-edge NEXAFS comparison, in Figure 4 shows a very small peak between the photon energy ranges for Cu(I) [931.9–933.4 eV] and Cu(II) [930.5–931.2 eV] for the CIS nanoparticle surfaces synthesized by the present method, as reported in the transition metal sulfide literature and mirrored in the ground bulk CIS (roquesite) spectrum.<sup>26</sup> The position of this peak near 931.6 eV, might suggest that quantum confinement lowers the Cu d-like LUMO energy. Both the SXPS and NEXAFS data clearly show good passivation of the CIS QD surfaces.

**Figure 4:** NEXAFS of roquesite and core CIS QDs

The hypothesis of Zn<sup>2+</sup> replacing Cu(I) and In(III) near the surface for CIS/ZnS QDs has been put forward by Park *et al.*, and Manna *et al.*,<sup>22</sup> Manna *et al.*, suggest that the extraction of copper will be favorable for Zn<sup>2+</sup> due to the Cu-S bond being weaker than In-S, as well as the Zn substitution for Cu being previously shown to be energetically favorable.

To investigate this, we performed a ToF-SIMS depth profile for Cu, In and Zn, on a freshly-fractured surface of synthetic roquesite, after surface modification using Zn(Ac)<sub>2</sub>. The depth profile, shown in Figure 5, shows a significant enhancement of Zn and Cu and correlated reduction in In secondary ion yield near the surface, with respect to the bulk. This suggests that, in contrast to the above expectation, Zn exchange for In is dominant in the surface layers. Simultaneously, the surface layer may contain a significant number of In vacancies, into which Zn may substitute. Certainly, a more detailed study is required, including the monitoring of solution species during the surface reaction with Zn(Ac)<sub>2</sub> solution coupled with further surface spectroscopy, for the full mechanism to be elucidated.

**Figure 5:** ToF-SIMS depth profile for Zn(Ac)<sub>2</sub>-treated synthetic roquesite surface

The form of Zn in the surface layers of Zn-exchanged QDs, however, is clear from the associated XPS analysis of the treated surfaces. Both the Zn LMM Auger electron and Zn 2p 3/2 photoelectron spectrum were collected during laboratory and synchrotron XPS measurements. These spectra are presented in Figures 6 and 7, respectively. The Zn LMM Auger position near 989.8 eV kinetic energy (Figure 6) is clearly indicative of a ZnS bonding environment. Indeed, the Zn LMM position is closely similar to that found by Bär *et al.*,<sup>27</sup> for the initial formation of ZnS/Zn(S, O) buffer layers chemically-deposited on CIS thin film solar absorbers. The Zn 2p 3/2 photoelectron has a much lower kinetic energy (approximately 75 eV, with the 1100 eV photon energy used in the SXPS experiment) and is hence more surface sensitive. As Figure 6 shows, there is evidence of both a ZnS and ZnO or Zn(OH)<sub>2</sub> chemical environment near the surface.

From a spectroscopic viewpoint, a model of the Zn treated CIS QD system may be presented, in which Zn exchanges with In (predominantly, the filling of In vacancies may also occur) in the CIS surface layers with Zn now tetrahedrally co-ordinated with S in the chalcopyrite structure. In the topmost monolayers, excess Zn may oxidize to, or deposit as, Zn(OH)<sub>2</sub>/ZnO species.

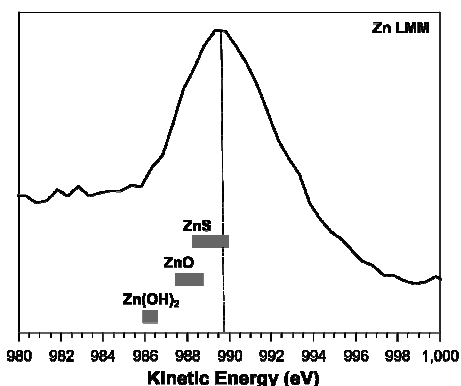


Figure 6: LMM Auger spectra for ZnS

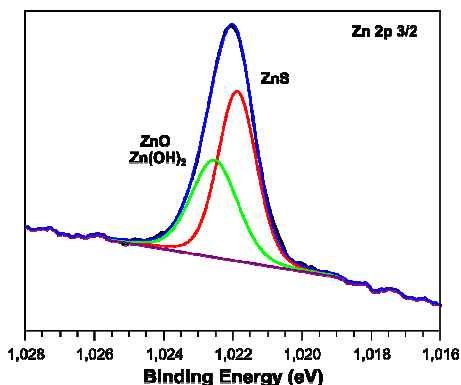


Figure 7: Zn 2p 3/2 XPS spectra for CIS QDs

#### Preliminary spectro-electrochemical analysis

Since CIS QDs have been previously recognised as useful sensitizers in photovoltaics, we measured the photocurrents of the as-prepared CIS QDs on a TiO<sub>2</sub> photoanode. The photocurrents of CIS QDs on TiO<sub>2</sub> were measured as a function of time and can be found in the supporting information (SP 2). We saw no difference in photocurrents between both the core CIS and CIS/ZnS QDs. These measurements used an Ag/AgCl reference electrode, platinum electrode and saline electrolyte in a photoelectrochemical cell (PEC). The TiO<sub>2</sub> films were immersed in CIS QD suspensions overnight and changed from white to a dark yellow color. CIS-sensitized electrodes exhibited initial photocurrents five times higher than that of bare TiO<sub>2</sub>. After electrochemical treatment the electrodes returned to white coloration. This is due to TiO<sub>2</sub> being a strong photo-oxidizing agent, oxidizing the CIS QDs. The decreasing photocurrents are evidence of the particles being oxidized on the surface. We recognize that stability is an issue and for these particles to be used for photovoltaics the oxidation of the particles would need to be improved. Therefore, future work is to try to lower the oxidation of the QDs by applying a buffer layer such as CdS.

#### Conclusion

We have found a new, straightforward and "green" method for the synthesis of optically stable CIS QDs. The effective band-gap can be adjusted by zinc cation exchange. Previous studies have suggested that the exchange of Cu for In is favorable. However, for the first time we have proven that In is replaced by Zn in a partial cation exchange. While some Cu may also be

replaced, ToF-SIMS depth profile measurements have confirmed the exchange of In is favorable. Furthermore, photocurrent measurements have shown the possibility for a photovoltaic system. Future work includes in-depth spectroscopic studies including quantum yields, lifetime measurements, and extended studies on the application for the prevention of oxidation for photovoltaic devices.

#### Experimental Section

##### Materials

Indium (III) Chloride InCl<sub>3</sub> 98%, Copper Acetate Cu(Ac)<sub>2</sub> 98%, Mercaptoacetic acid TGA 98%, Sodium sulfide Na<sub>2</sub>S 98%, Zinc Acetate Zn(Ac)<sub>2</sub> 99%, were all purchased from Sigma-Aldrich. Aeroxide TiO<sub>2</sub> P25 nanoparticles were supplied by EVONIK (Degussa) Industries. 1.5 cm x 1.5 cm ITO coated glass electrodes were supplied by Präzisions Glas & Optik GmbH.

##### Synthesis of core CIS QDs

CuInS<sub>2</sub> nanocrystals were synthesized similar to a method described by Meng et al.,<sup>21</sup> with some modification. In a typical synthesis, 0.5 mL Cu(Ac)<sub>2</sub> (0.125 M) and 0.5 mL InCl<sub>3</sub> (0.125 M) aqueous solutions were injected into 37.5 mL of degassed, deionized water with steady stirring at room temperature. 0.25 mL of stabilizing agent mercaptoacetic acid (1:5) aqueous solution was then injected to the mixture. Upon injection of the stabilizing agent the clear solution changed to black before changing back to clear. The pH of the solution was then neutralized by adding approximately 1 mL of NaOH. Once the solution was neutralized (pH 7), 0.25 mL of Na<sub>2</sub>S (0.5 M) was injected causing an immediate deep red color change. The quantum dot solution was then transferred to a Teflon-lined dialysis chamber to remove the unreacted products such as excess mercaptoacetic acid. In the case of ZnS cation exchange, the quantum dots were taken as prepared. In the case of further characterization, the CuInS<sub>2</sub> QDs could be precipitated as a powder by ethanol. The precipitate was isolated by centrifugation and washed several times with ethanol. Once precipitated and washed the CuInS<sub>2</sub> powder was then dried in a vacuum desiccator for 1-2 hours. The obtained CuInS<sub>2</sub> powder was then used for XRD, TEM, XPS and NEXAFS.

##### Cation Exchange of QDs with ZnS

To obtain a wavelength of 610 nm, Zn(Ac)<sub>2</sub> (6 mM) was added to the QDs. The new mixture was then heated to 70 °C for 24 hours where over the first 4 hours the solution changed from red to an orange-yellow color. The intensity of the color change depended on the amount of zinc added. After the 24 hours had elapsed, the QDs were purified the same way as the core CuInS<sub>2</sub>. The CuInS<sub>2</sub>/ZnS QDs were successfully obtained. Variation of the zinc concentration showed PL peak shifts from 610 to 725 nm (table 1).

**Table 1: Variation of ZnS concentration**

| ZnS concentration (mM) | ZnS tuning wavelengths |                       |
|------------------------|------------------------|-----------------------|
|                        | Wavelength (nm)        | Wavelength shift (nm) |
| 0                      | 725                    | N/A                   |
| 3                      | 660                    | 65                    |
| 4                      | 640                    | 85                    |
| 5                      | 625                    | 100                   |
| 6                      | 610                    | 115                   |

**Quantum dot sensitized photo-electrodes**

TiO<sub>2</sub> paste (see supporting information for paste formation) was applied to the surface of an ITO coated glass slides (Präzisions Glass & Optik GmbH) via doctor blade technique and sintered at 450 °C for 2 hours. The TiO<sub>2</sub> photoelectrodes were immersed in a solution of CuInS<sub>2</sub> QDs for 24 hours changing the color of the electrodes from white to dark red. The color of the electrodes after coating depended on what concentration of zinc was used. The higher the concentration of zinc, the lighter the solution hence electrodes appeared.

**Characterization**

Photoluminescence spectroscopy measurements were carried out on an Edinburgh Instruments Fluorometer FLS980. Conventional XPS measurements were undertaken using monochromatised Al K $\alpha$  X-rays (300 W) in a Kratos Axis-Ultra spectrometer (10 eV analyzer pass energy). The analysis spot size was ~300 x 700  $\mu$ m. Core electron binding energies are given relative to an adventitious hydrocarbon C 1s binding energy of 284.8 eV. Time-of-Flight Secondary Ion Mass Spectrometry (ToF-SIMS) was used to perform elemental depth profiles on Zn treated (exchanged) surfaces of synthetic CuInS<sub>2</sub> (roquesite). The ToF-SIMS instrument was a Physical Electronics TRIFT V NanoToF. Depth profiles were conducted using a single Au 30keV LMIG source operating in pulsed and continuous modes for analysis and sputtering cycles respectively.

**Australian Synchrotron characterization**

The synchrotron X-ray photoelectron spectroscopic (SXPS) and Near Edge X-ray Absorption Fine Structure (NEXAFS) spectroscopic measurements were carried out at Beamline 14ID at the Australian Synchrotron using the soft X-ray spectroscopy end-station. BL14ID is a wide range, grating monochromator beam-line, with an elliptically polarizing undulator source. On BL14ID, the beam linewidth would have been less than 0.1 eV at 600 eV, 0.2 eV at 1100 eV and 0.3 eV at 1500 eV. The soft X-ray end-station, constructed by OmniVac and Pre-Vac, is equipped with a SPECS Phoibos 150 electron energy analyzer and an OmniVac UHV-compatible partial yield detector based on a multichannel plate behind retarding grids. Electron analyzer pass energies of 5, 10 or 20 eV for narrow range spectra. Binding energies are reported relative to a Au 4f<sub>7/2</sub> value of 84.0 eV for a Au metal foil, mounted adjacent to the sample on the analysis chamber stage. NEXAFS spectra are shown with the true photon energy established via the absorption current monitored concomitantly by a reference

metal mesh in the beam-line, and normalized by the flux incident on a Au mesh also in the beam-line. The experimental setup allows for the simultaneous collection of total electron yield (TEY), Auger electron yield via the electron analyzer (AEY) and fluorescence yield (FY). Vacuum in the analytical chamber was < 3 x 10<sup>-10</sup> torr during all measurements.

Confirmatory, lab-based XPS measurements were also undertaken using monochromatized Al K $\alpha$  X-rays (300 W) in a Kratos Axis-Ultra spectrometer (10 eV analyzer pass energy). The analysis spot size was ~300 x 700  $\mu$ m. Core electron binding energies are given relative to an adventitious hydrocarbon C 1s binding energy of 284.8 eV.

**Acknowledgements**

This work was performed in part at the South Australian node of the Australian National Fabrication Facility (ANFF), a company established under the National Collaborative Research Infrastructure Strategy to provide nano and micro-fabrication facilities for Australia's researchers. Another part of this research was conducted and funded by the Australian Research Council Centre of Excellence in Convergent Bio-Nano Science and Technology (project number CE140100036). The synchrotron-based measurements were undertaken on the Soft X-ray Spectroscopy beamline at the Australian Synchrotron, Victoria, Australia. Laboratory XPS analyses were performed at the South Australian Node of the Australian Microscopy and Microanalysis Research Facility (AMMRF).

**Notes and references**

<sup>a</sup>Ian Wark Research Institute, University of South Australia, Mawson Lakes, 5095 SA, Australia, E-mail: thomas.nann@unisa.edu.au

<sup>b</sup>Adelaide Microscopy, The University of Adelaide, Adelaide, 5000 SA, Australia

<sup>c</sup>ARC Centre of Excellence in Convergent Bio-Nano Science

† Thomas J. Macdonald and Yatin J. Mange contributed equally to the research in this manuscript. Melissa Dewi carried out the transmission electron microscopy. Aoife McFadden completed the study on the bulk material at the University of Adelaide. William Skinner carried out the x-ray photon spectroscopy and synchrotron studies at the Australian Synchrotron facilities, Victoria, Australia. Thomas J. Macdonald, William Skinner and Thomas Nann were mainly responsible for the writing of the manuscript.

Electronic Supplementary Information (ESI) available: [details of any supplementary information available should be included here]. See DOI: 10.1039/b000000x/

1. T. Pons, E. Pic, N. Lequeux, E. Cassette, L. Bezdetnaya, F. Guillemin, F. Marchal, and B. Dubertret, *ACS Nano*, 2010, **4**, 2531–2538.
2. D.-E. Nam, W.-S. Song, and H. Yang, *J Mater Chem*, 2011, **21**, 18220–18226.
3. H. Zhong, S. S. Lo, T. Mirkovic, Y. Li, Y. Ding, Y. Li, and G. D. Scholes, *ACS Nano*, 2010, **4**, 5253–5262.
4. J. Park and S.-W. Kim, *J Mater Chem*, 2011, **21**, 3745–3750.

5. T.-L. Li, Y.-L. Lee, and H. Teng, *J. Mater. Chem.*, 2011, **21**, 5089–5098.
6. F. Dubois, B. Mahler, B. Dubertret, E. Doris, and C. Mioskowski, *J Am Chem Soc*, 2006, **129**, 482–483.
7. B.-K. Pong, B. L. Trout, and J.-Y. Lee, *Langmuir*, 2011, **24**, 5270–5276.
8. H. T. Uyeda, I. L. Medintz, J. K. Jaiswal, S. M. Simon, and H. Mattoussi, *J Am Chem Soc*, 2011, **127**, 3870–3878.
9. V. S. Gurin, *Colloids Surf. -Physicochem. Eng. Asp.*, 1998, **142**, 35–40.
10. S. L. Castro, S. G. Bailey, R. P. Raffaella, K. K. Banger, and A. F. Hepp, *Chem. Mater.*, 2003, **15**, 3142–3147.
11. J. J. Nairn, P. J. Shapiro, B. Twamley, T. Pounds, R. von Wandruszka, T. R. Fletcher, M. Williams, C. M. Wang, and M. G. Norton, *Nano Lett.*, 2006, **6**, 1218–1223.
12. R. Xie, M. Rutherford, and X. Peng, *J. Am. Chem. Soc.*, 2009, **131**, 5691–5697.
13. M.-Y. Chiang, S.-H. Chang, C.-Y. Chen, F.-W. Yuan, and H.-Y. Tuan, *J. Phys. Chem. C*, 2011, **115**, 1592–1599.
14. H. Nakamura, W. Kato, M. Uehara, K. Nose, T. Omata, S. Otsuka-Yao-Matsuo, M. Miyazaki, and H. Maeda, *Chem. Mater.*, 2006, **18**, 3330–3335.
15. D. Pan, L. An, Z. Sun, W. Hou, Y. Yang, Z. Yang, and Y. Lu, *J. Am. Chem. Soc.*, 2008, **130**, 5620–5621.
16. H. D. Duong, C. V. G. Reddy, J. I. Rhee, and T. Vo-Dinh, *Sens. Actuators B Chem.*, 2011, **157**, 139–145.
17. L. Li, T. J. Daou, I. Texier, T. T. Kim Chi, N. Q. Liem, and P. Reiss, *Chem. Mater.*, 2009, **21**, 2422–2429.
18. D. H. Son, S. M. Hughes, Y. Yin, and A. Paul Alivisatos, *Science*, 2004, **306**, 1009–1012.
19. D.-E. Nam, W.-S. Song, and H. Yang, *J. Colloid Interface Sci.*, 2011, **361**, 491–496.
20. S. Peng, F. Cheng, J. Liang, Z. Tao, and J. Chen, *J. Alloys Compd.*, 2009, **481**, 786–791.
21. X. Hu, Q. Zhang, X. Huang, D. Li, Y. Luo, and Q. Meng, *J Mater Chem*, 2011.
22. L. De Trizio, M. Prato, A. Genovese, A. Casu, M. Povia, R. Simonutti, M. J. P. Alcocer, C. D'Andrea, F. Tassone, and L. Manna, *Chem. Mater.*, 2012, **24**, 2400–2406.
23. S. Liu, H. Zhang, Y. Qiao, and X. Su, *RSC Adv.*, 2012, **2**, 819–825.
24. J. Zhang, R. Xie, and W. Yang, *Chem Mater*, 2011, **23**, 3357–3361.
25. W. M. Skinner, C. A. Prestidge, and R. S. C. Smart, *Surf. Interface Anal.*, 1996, **24**, 620–626.
26. A. N. Buckley, W. M. Skinner, S. L. Harmer, A. Pring, R. N. Lamb, L.-J. Fan, and Y. Yang, *Can. J. Chem.*, 2007, **85**, 767–781.
27. M. Bar, A. Ennaoui, J. Klaer, T. Kropp, R. Saez-Araoz, N. Allsop, I. Lauer mann, H.-W. Schock, and M. C. Lux-Steiner, *J. Appl. Phys.*, 2006, **99**, 123503–9.
- 1 Citations here in the format A. Name, B. Name and C. Name, *Journal Title*, 2000, **35**, 3523; A. Name, B. Name and C. Name, *Journal Title*, 2000, **35**, 3523.